Physics of Plasmas

Indirect energy transfer channel between fast ions via nuclear elastic scattering observed on the large helical device

Cite as: Phys. Plasmas **29**, 092502 (2022); https://doi.org/10.1063/5.0097720
Submitted: 01 May 2022 • Accepted: 11 August 2022 • Published Online: 12 September 2022

H. Matsuura, K. Kimura, D. Umezaki, et al.

Physics of Plasmas ARTICLE scitation.org/journal/php

Indirect energy transfer channel between fast ions via nuclear elastic scattering observed on the large helical device

Cite as: Phys. Plasmas **29**, 092502 (2022); doi: 10.1063/5.0097720
Submitted: 1 May 2022 · Accepted: 11 August 2022 ·
Published Online: 12 September 2022

H. Matsuura,[1,a)] K. Kimura,[1] D. Umezaki,[1] K. Ogawa,[2,3] M. Isobe,[2,3] Y. Kawamoto,[2] T. Oishi,[2,3] M. Goto,[2,3] N. Tamura,[2,3] M. Osakabe,[2,3] T. Nishitani,[4] and S. Sugiyama[5]

AFFILIATIONS

[1]Department of Applied Quantum Physics and Nuclear Engineering, Kyushu University, 744 Motooka, Fukuoka 819-0395, Japan
[2]National Institute for Fusion Science, National Institutes of Natural Sciences, 322-6 Oroshi-cho, Toki 509-5292, Japan
[3]Department of Fusion Science, The Graduate University for Advanced Studies, Sokendai, 322-6 Oroshi-cho, Toki 509-5292, Japan
[4]Graduate School of Engineering, Nagoya University, Furo-cho, Chikusa-ku, Nagoya 464-8603, Japan
[5]National Institutes for Quantum and Radiological Science and Technology, Rokkasho, Aomori 039–3212, Japan

[a)]**Author to whom correspondence should be addressed**: matsuura@kyudai.jp

ABSTRACT

An energy transfer phenomenon between energetic ions, which cannot be explained only considering the Coulomb scattering process, was observed on a large helical device (LHD). This phenomenon often occurs in fusion reactivity enhancement and fast-ion slowing-down process that can be observed as a delay in the decay time of the $D(d,n)^3He$ neutron generation rate. The transferred energy required to induce such a reactivity enhancement or delay in the fast-ion slowing-down time (neutron decay time) was examined based on the Boltzmann–Fokker–Planck analysis in which a discrete energy transfer process, called nuclear elastic scattering (NES), is included. It was shown that even though the cross section of the NES is smaller than that of the Coulomb scattering, enough knock-on population appears in the energetic region in ion distribution function to induce the observable NES effects; thus, enough energy is transferred from beam ions to fast component of bulk ion distribution function indirectly and the transferred energy per unit time via NES is comparable to the Coulomb scattering rate. This study analytically demonstrates that the observed phenomena on LHD can be explained smoothly by considering the alternative indirect energy transfer channel between energetic ions, which can be comparable with the one via Coulomb scattering.

I. INTRODUCTION

In a thermonuclear fusion reactor, fusion born non-thermal ions must sustain the bulk plasma pressure through collisional power transfer, i.e., nuclear burning. Energetic ions play an essential role in determining important physical information for nuclear burning. The Coulomb scattering process is the dominant energy transfer process that takes place between charged particles in a thermonuclear fusion reactor. However, nuclear elastic scattering (NES) contributes to the energy transfer process and can bring certain modifications to the slowing-down behavior as the ion energy increases.[1–3] The cross section of the NES is defined by subtracting the Coulomb scattering contribution from the experimentally measured one.[4] Therefore, the actual energy transfer mechanism can be accurately reproduced only after the NES contribution is incorporated into the analysis in addition to the Coulomb contribution. NES induces a modification of the ion velocity distribution functions. When the ion velocity distribution function is modified from Maxwellian, the emission spectrum of the fusion products changes its shape from that of a Gaussian distribution.[5] A non-Gaussian energetic component in the T(d,n)α neutron emission spectrum was observed in JET.[6,7] This component is created by T(d,n)α reactions between the energetic recoil (knock-on) components in the deuteron and triton distribution functions owing to the energy transfer phenomena via NES. The NES effect on the fast-ion slowing-down process has also been observed in the large helical device (LHD).[8] The enhancement of the $D(d,n)^3He$ reactivity due to NES was also observed.[9] The NES occurs in a high-temperature plasma operation. The NES effect may be negligible in several stages in the DT fusion reactor operation; however, in some other stages, e.g., in

D^3He plasma, its effect can influence nuclear burning.[2,3] Therefore, it is essential to understand the NES features in burning plasma and validate the numerical approaches to develop a thermonuclear fusion reactor.

NES is a non-Coulomb scattering process in which a large fraction of the ion energy is transferred during a single scattering event. As a result of this, the energetic ions lose their energy faster (transferred energy per unit time increases) than when only the Coulomb scattering process[2,3,10] is considered. In contrast, energetic ions are continuously produced via NES process of energetic ions owing to the accumulation of discrete high-energy transfer processes from energetic to thermal ions. Through this process, the number of ions in the energy range where recoil ions appear is enhanced, and the slowing-down time is delayed.[8] The fast protons do not much interact with fast deuterons via NES and do not provide distortion of the fast deuteron distribution function directly; rather, the fast protons interact with bulk deuterons via NES and create a knock-on population in the fast deuteron distribution function. As a result, fast proton energy is transferred to fast component of the deuteron distribution function indirectly. Some recoil ions also lose their energy through the Coulomb scattering process. Others may lose their energy through NES and create recoil ions again in a significantly higher energy range. Thus, energetic ions can deliver their energy through NES to the lower energy ions distinctively from Coulomb scattering. Therefore, it is essential to understand these processes to achieve stable and efficient nuclear burning in future fusion reactors. However, the quantitative experimental confirmation has not been extensively studied. This study attempted to understand these processes by observing the delay in the slowing-down time of energetic ions that appear as a delay in the neutron decay time of the neutron generation rate.

The LHD in the National Institute for Fusion Science is equipped with negative-ion neutral beam injectors (NBI) with beam energies ranging from 160 to 190 keV.[11,12] According to the general elastic scattering theory, a proton of 180 keV can transfer a maximum energy of 160 keV to a stationary deuteron in a single elastic scattering interaction determined depending on the scattering angle in the center of mass (CM) systems. The most probable energy transferred is approximately 80 keV, as the target ion is nearly stationary. This study focuses on the deuterons injected by the positive-NBI with an energy of 50−60 keV to observe the energy transfer process via NES induced by protons ranging between 160 and 190 keV. If a meaningful energy transfer due to a large-angle scattering occurs as previously predicted, the slowing-down time of the 50−60 keV deuterons, which appears as a delay in the neutron decay time, would increase. In the experiment, the decay time of the neutron generation rate produced by the beam deuterium is observed.

This study evaluates the transferred energy per unit time via NES and quantitatively examines the phenomena observed in the LHD. The Fokker–Planck (FP) equation was used to analyze the time evolution of the velocity distribution function through the Coulomb scattering process. The FP equation was introduced to treat small-angle scattering processes, such as Coulomb scattering. The Boltzmann equation was used to examine the time variation of the velocity distribution function. The Boltzmann−Fokker−Planck (BFP) model[10,13] was developed, where small-angle Coulomb and large-angle scattering (NES) processes were considered. Based on the BFP simulation, the amount of indirect transferred energy from energetic protons to slowing-down deuterons through NES was evaluated. The transferred energy evaluated is ensured by comparing the BFP simulations with the DD reactivity enhancement and the neutron decay time observed in the LHD, and the transferred energy via NES is also compared with the one through Coulomb scattering. The measured data were explained by considering the knock-on fast ion population that is produced by the indirect transferred energy via NES. A numerical prediction of the NES effect, which is expected to appear in future fusion devices, is also demonstrated.

II. EXPERIMENTAL APPARATUS

Figure 1 summarizes the performances of NBIs, i.e., injected particle species, approximate port-through beam powers and energies, in the LHD for specific shots (a) #172066 and #172068, (b) #164881 and #164874 used in this study. Here, the port-through power is defined as a sum of deposition and shine-through powers. In the experiment, deuterium plasma was heated using NBIs and electron cyclotron resonance heating (ECH). Three negative-hydrogen (H) beam (NBI#1, 2, and 3) and two positive-deuterium (D) beam (NBI#4 and 5) injectors were used for shots #177066 and #177068, and one negative-hydrogen (H) beam (NBI#1), two negative-deuteron (D) beam (NBI#2 and 3) and two positive-deuterium (D) beam (NBI#4 and 5) injectors for

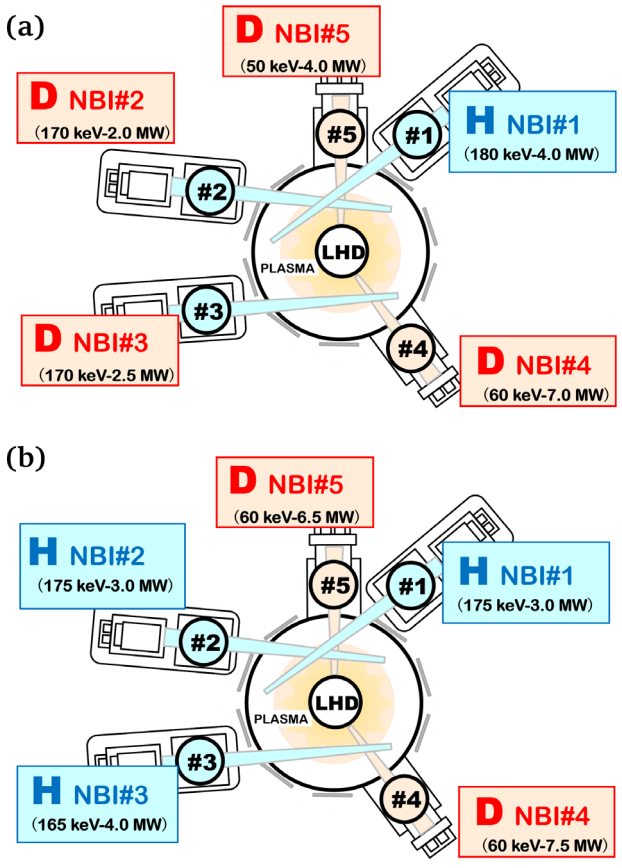

FIG. 1. Schematics of the neutral beam injector patterns in large helical device with approximate beam energies and port-through powers for typical shots (a) #172066 and #172068, and (b) #164874 and #164881.

shots #164874 and #164881. NBI#1, 2, and 3 are the injectors that are directed tangentially toward the axis of the toroidal magnetic field, with the negative-ion sources providing fast hydrogens or deuterium at energies of approximately 170−190 keV with a port-through power of approximately 2−4 MW (tangential injectors). NBI#4 and 5 are perpendicular to the magnetic axis, with positive-ion sources of approximately 50−60 keV deuterium with a port-through power of approximately 4−8 MW. High-purity (enriched) H was prepared in tangential injectors for this experiment. The deuterium atomic ratio contained in the hydrogen beam as an impurity was suppressed to be less than 1 ppm. The neutron generation rates were estimated to be the average value of the three ^{235}U fission chambers (FCs). One of the fission chambers was placed on the magnetic axis, and the remaining two fission chambers were placed on different sides of the LHD vacuum vessel. A magnetic axis $R_{ax} = 3.6$ m and a toroidal magnetic field $B_t = 2.75$ T (counterclockwise direction) were maintained throughout the experiment.

III. ANALYSIS MODEL

In the BFP model, a uniform deuterium plasma accompanied by deuterium and hydrogen beam injections is assumed. Three kinds of ion species were considered, i.e., field deuteron with Maxwellian distribution function, fast deuteron, beam proton, and electrons (see Table I). The fast deuterons are divided into energetic components owing to beam injection (beam deuteron) and recoil (knock-on) deuteron created by NES. The neutron generation by the D(d,n)^{3}He reaction between the fast and field deuterons is considered. The time-dependent BFP equation for fast deuteron (proton), i.e., k = fast deuteron or beam proton, is given by

$$\frac{df_k}{dt} = \sum_j \left(\frac{\partial f_k}{\partial t}\right)_j^{\text{Coulomb}} + \sum_i \left(\frac{\partial f_k}{\partial t}\right)_i^{\text{NES}} + \frac{1}{v^2}\frac{\partial}{\partial v}\left(\frac{v^3 f_k}{2\tau_c^{*k}(v)}\right) + S_k(t,v) - L_k(t,v), \tag{1}$$

where $f_k(t,v)$ is the time-dependent isotropic velocity distribution function of the species k. The first term on the right-hand side of Eq. (1) represents the effect of the Coulomb collisions.[14] The summation is taken over all background species, i.e., j = field deuteron, fast deuteron, beam proton, and electron. Thus, the Coulomb collision term is nonlinear retaining collisions between ions of the same species. The second term accounts for the NES of species k.[10] This study considers NES between (1) fast deuteron and field deuteron, (2) fast deuteron and fast deuteron, (3) beam proton and field deuteron, and (4) beam proton and fast deuteron, as (k, i) = (fast deuteron, field deuteron), (fast deuteron, fast deuteron), (beam proton, field deuteron), and (beam proton, fast deuteron). The second term accounts for the NES,

$$\left(\frac{\partial f_k}{\partial t}\right)_i^{\text{NES}} = \frac{2\pi}{v^2}\int_0^\infty v' f_{k'}(v') \int_0^\infty v_i f_i(v_i) P(v' \to v|v_i) \times \int_{|v'-v_i|}^{v'+v_i} v_r'^2 \sigma_{\text{NES}}(v'_r) dv'_r dv_i dv' - \frac{2\pi}{v} f_k(v) \int_0^\infty v_i f_i(v_i) \int_{|v-v_i|}^{v+v_i} v_r^2 \sigma_{\text{NES}}(v_r) dv_r dv_i, \tag{2}$$

where $v'_r = |\boldsymbol{v}' - \boldsymbol{v}_i|$ and $v_r = |\boldsymbol{v} - \boldsymbol{v}_i|$, k = beam proton (or fast deuteron), and k' = beam proton (or sum of fast and field deuterons). The first term in Eq. (2) represents the rate of scattering ions into the velocity interval dv due to NES from the overall velocity space. The second term in Eq. (2) denotes the rate of scattering out of ions from the velocity interval dv due to NES. Suppose the scattering event of ion species k which has the velocity $\boldsymbol{v}'$ by ion species i which has the velocity $\boldsymbol{v}_i$. If the incident ion is scattered through an angle φ, then

$$\cos\varphi = \frac{|\boldsymbol{v}|^2 - |\boldsymbol{V}_C|^2 + |\boldsymbol{V}|^2}{2|\boldsymbol{V}_C||\boldsymbol{V}|}. \tag{3}$$

Here, $\boldsymbol{v}$ and $\boldsymbol{V}$ represent the velocities of ion species k after the scattering in the laboratory and the center of mass (CM) systems, respectively, $\boldsymbol{V}_C$ the velocity of center of mass and φ the angle between $\boldsymbol{V}_C$ and $\boldsymbol{V}$. The NES cross sections are taken from the work of Cullen and Perkins[15] (see Fig. 2). For the deuterium beam, it was shown that if the target ion species are triton and ^{3}He, the angular distribution of NES is, to a certain extent, backward-peaked.[14,15] In this case, the assumption of isotropic scattering may underestimate the NES effect on plasma properties. However, for proton or deuteron targets, the isotropic scattering assumption would be a good approximation.[15,16] This study assumed isotropic scattering for NES in the center of mass

TABLE I. Charged-particle species considered in Boltzmann−Fokker−Planck simulation.

Species	Distribution functions	
Electron	Maxwellian	Field particle
Field deuteron	Maxwellian	
Fast deuteron	$f_D(v)$ $(\equiv f_D^{\text{beam}}(v) + f_D^{\text{recoil}}(v))$	Energetic particle
Beam proton	$f_p(v)(\equiv f_p^{\text{beam}}(v))$	

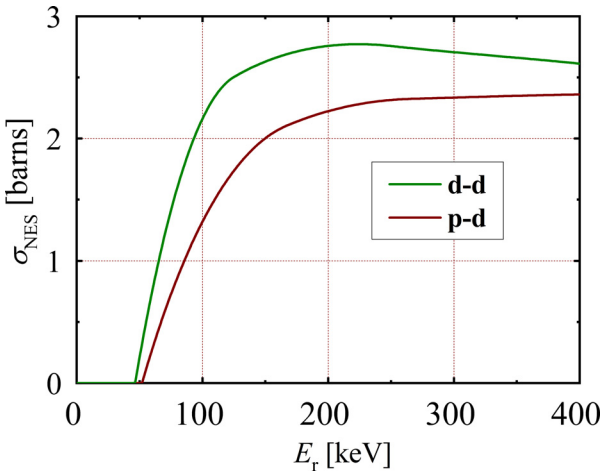

FIG. 2. Cross sections of deuteron-deuteron and proton-deuteron NES as a function of the relative energy of reactants.

systems. In this case, the probability distribution function P (i.e., probability that the injected beam ion which has the speed v' is scattered into the speed region v owing to the NES with background ion, which has speed v_i) can be written as follows:

$$P(v' \to v|v_i)dv = \begin{cases} \dfrac{|\boldsymbol{v}|}{2|\boldsymbol{V}_C||\boldsymbol{V}|}dv & \text{for } |\boldsymbol{V}_C - \boldsymbol{V}| \le v \le |\boldsymbol{V}_C + \boldsymbol{V}|, \\ 0 & \text{otherwise.} \end{cases} \tag{4}$$

The third term on the right-hand side of Eq. (1) represents the diffusion in velocity space due to thermal conduction. In this study, the velocity dependence of the particle and energy confinement times was incorporated into the analysis using the dimensionless parameter γ following the Bittoni's treatment[17] to reflect the particle and energy losses during particle motion in a three-dimensional magnetic confinement configuration to a uniform plasma model. Bittoni's treatment is given by

$$\tau^{*k}_{c(p)}(v) = \begin{cases} C^k_{c(p)}\tau^k_{c(p)} & \text{when } v < v^k_{th}, \\ C^k_{c(p)}\tau^k_{c(p)}\left(\dfrac{v}{v^k_{th}}\right)^{\gamma} & \text{when } v \ge v^k_{th}. \end{cases} \tag{5}$$

Here, v^k_{th} is the thermal velocity of ion species k, and the coefficient C^k_c(or C^k_p) is determined so that the velocity-integrated energy (or particle) loss rate becomes $(3/2)n_kT_i/\tau^k_c$(or n_k/τ_p) for each ion species. The asterisk in Eq. (5) implies that the variable is a function of the velocity. Considering both energy loss mechanisms due to thermal conduction and particles transport loss from the plasma, the confinement time for conduction loss time τ^k_c is determined using the global energy confinement time τ_E to satisfy the following relation for each species:

$$\frac{(3/2)n_kT_i}{\tau_E} = \frac{(3/2)n_kT_i}{\tau^k_c} + \int \frac{(1/2)m_kv^2_k}{\tau^{*k}_p(v)} f_k(v_k)d\vec{v}_k. \tag{6}$$

The high exponent γ chosen ensures a rapid increment of energy and particle confinement times for energetic particles compared with the thermal components. As discussed in Ref. 10, as in the usual fusion plasma, the γ would not be an influential parameter. This study assumed $\gamma = 6$ throughout the simulation. The γ dependencies on the NES effects are discussed in Sec. IV. The particle confinement time for protons (tangential injection to the magnetic field) is assumed as 0.5 s, referencing the work of Nuga *et al.*[18] The confinement time for deuterons (vertical injection to the magnetic field) is determined to be consistent with the present experiment.

The source $[S_{D(p)}(v)]$ and loss $[L_{D(p)}(v)]$ terms for beam deuteron and proton are described as follows:

$$S_{D(p)}(t,v) - L_{D(p)}(t,v) = \frac{S_{D(p)}}{4\pi v^2}\delta(v - v^{beam}_{D(p)}) - \frac{f_{D(p)}(t,v)}{\tau_p(v)}. \tag{7}$$

Here, $v^{beam}_{D(p)}$ is the speed of the beam-injected deuteron (proton). The beam injection rate $S_D(S_p)$ is determined using beam injection energy $E^{NBI}_{D(p)}$ and power $P^{NBI}_{D(p)}$, and plasma volume V as $S^{NBI}_{D(p)} = P^{NBI}_{D(p)}/E^{NBI}_{D(p)}V$. The plasma volume was taken as 30 m^3 throughout the simulations. The reaction rate coefficient of the D(d,n)^{3}He fusion reaction between fast and field deuterons is given by

$$\langle\sigma v\rangle_{D(d,n)^3He}(t) = \frac{4\pi}{n^{fast}_D n^{field}_D}\int dv_D v^2_D \varsigma(t,v_D) f^{field}_D(t,v_D) \tag{8}$$

with

$$\varsigma(t,v_D) = \frac{2\pi}{v_D}\int dv^{fast}_D v^{fast}_D f^{fast}_D(t,v^{fast}_D)\left[\int_{|v^{fast}_D - v_D|}^{v^{fast}_D + v_D} dv_r v^2_r \sigma_{DD}(v_r)\right]. \tag{9}$$

Here, v_r is the relative velocity of the beam and field deuterons, i.e., $v_r = |\boldsymbol{v}_{fast} - \boldsymbol{v}_{field}|$. The D(d,n)^{3}He fusion cross sections are taken from the work of Bosch and Hale.[19]

The transferred power from charged particle species k to j is evaluated using both velocity distribution functions obtained as follows:

$$P^{Coulomb}_{k\to j}(t) = \int -\left(\frac{dE_k}{dt}\right)_j 4\pi v^2 f_k(t,v)Vdv, \tag{10}$$

where $(dE_k/dt)_j$ is the energy loss rate of species k due to the Coulomb collisions with species j. The energy loss rate is given by

$$\left(\frac{dE_k}{dt}\right)_j = -\frac{Z^2_kZ^2_je^4\ln\Lambda}{\varepsilon^2_0 m_k v}\left[\frac{m_k}{m_j}\int_0^v f_j(t,x)x^2dx - v\int_v^\infty f_j(t,x)xdx\right]. \tag{11}$$

The transferred power from ion species k to i through NES is given by

$$P^{NES}_{k\to i}(t) = -\int \frac{1}{2}m_kv^2\left(\frac{\partial f_k}{\partial t}\right)^{NES}_i 4\pi v^2 Vdv. \tag{12}$$

IV. RESULTS AND DISCUSSION

A. Observation of attenuation feature of the neutron generation rate

In the experiment, the deuterium plasma was heated using ECH and NBIs (a pair of deuterium NBI#5 and one (or two) high-purity hydrogen NBI#1 (NBI#1 + 3) beams). Figure 3 shows a typical waveform pattern of a deuterium plasma discharge, i.e., # 172068, including the time evolutions of (a) the neutral beam heating powers for injectors NBI#1 (port-through and deposition powers), and #5 (port-through power), (b) the electron temperature at the radius $r = 0$ and $a/2$ (a is a minor radius of the LHD plasma), (c) the electron density at the radius $r = 0$ and $a/2$, and (d) the neutron generation rate measured by the fission chamber. After 4 s at the beginning of plasma discharge, deuterium beam injection (NBI#5) was terminated, whereas the hydrogen beams NBI#1 remained injected. After terminating NBI#5 at 4 s, the neutron generation rate by the D(d,n)^{3}He reaction gradually decreased. The authors focused on the decay time τ_n defined as the time after which the fast-thermal D(d,n)^{3}He reaction rate is reduced to $1/e$. The time evolutions of the normalized neutron generation rate for (i) w/o hydrogen beams, (ii) with NBI#1, and (iii) with NBI#+3 are plotted in Fig. 4. The neutron generation rates were normalized by the values when deuterium beam was terminated. The decay times when NBI#1 or NBI#1 + 3 (or w/o NBI#1) remain were estimated by least squares fitting and the errors were estimated by changing the time limits from 50 to 100 ms as 44.3 ± 0.8 and 46.8 ± 0.47

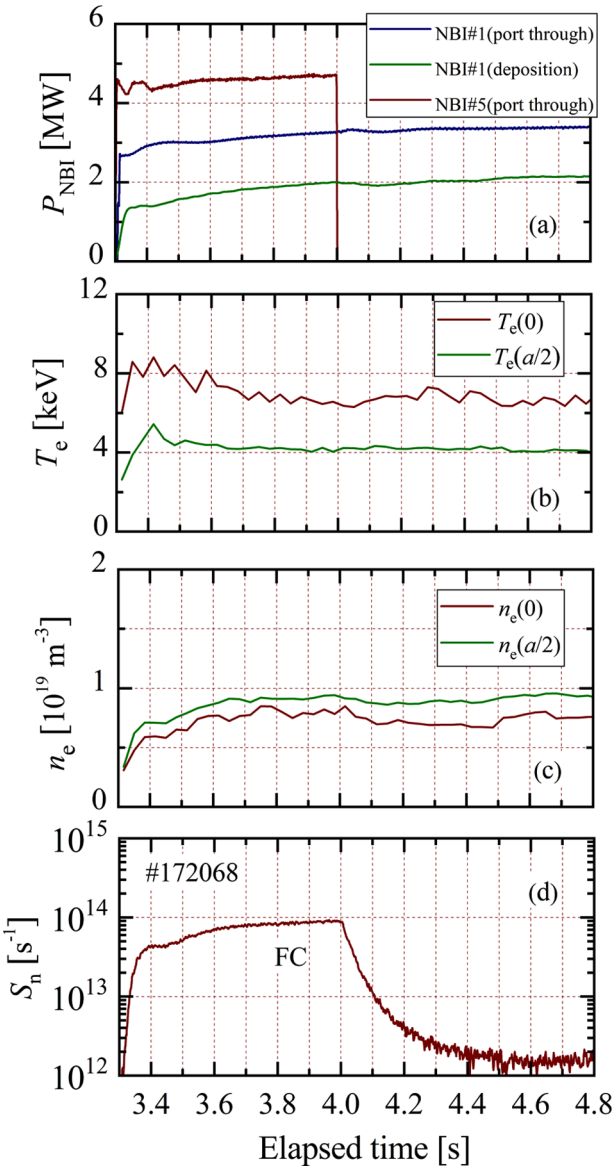

FIG. 3. Time evolution of the deuterium plasma discharge (shot no. #172068). (a) neutral beam heating powers for injectors NBI#1, and 5; (b) electron temperatures at r = 0 and a/2; (c) electron density at r = 0 and a/2; and (d) neutron generation rate detected by the fission chamber (FC).

(35.2 ± 0.13) ms, respectively. The injection power, time-averaged electron temperature, density from 4.0–4.1 s, and decay time for shots (i) and (ii) are summarized in Table II along with (iii) #164881. In the shot #164881, after 4.3 s at the beginning of plasma discharge, deuterium beam injection (NBI#5) was terminated, whereas the high-purity hydrogen beams NBI#1 + 3 remained injected. The ion temperature is approximately 2 keV in all shots. Since the theoretical scaling of the slowing-down time is $\tau_s \propto T_e^{3/2}/n_e$, no valid reason exists under the background plasma conditions to explain the difference in the neutron decay time.

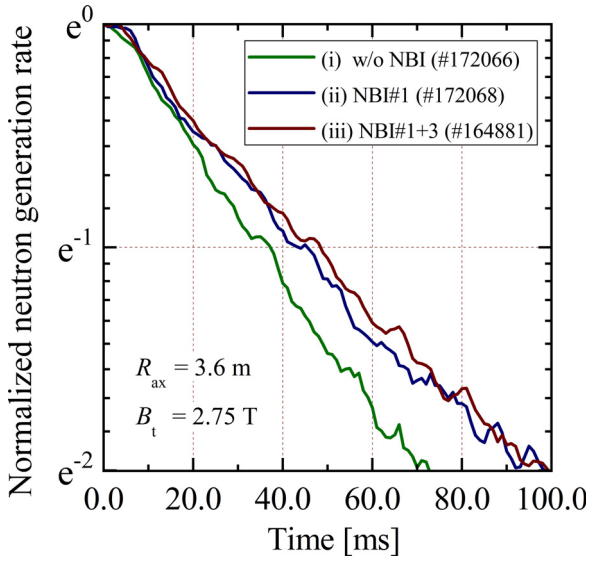

FIG. 4. Attenuation processes of the normalized neutron generation rates when (i) no hydrogen beams are injected (#172066), along with the shot when (ii) NBI#1 remained injected (#172068) and (iii) NBI#1 + 3 remained injected (#164881) as a function of the time after NBI#5 was terminated.

B. Evaluation of transferred power via NES and comparison with experiment

At first, we consider the situation when high-purity beam is injected into deuterium plasma to examine the net transferred power to create the knock-on tail in a deuteron distribution function. Figure 5 shows the time evolution of the (a) proton and (b) deuteron velocity distribution functions after a high-purity hydrogen beam is injected into the deuterium plasma. Here, $t = 0$ represents the time when a high-purity hydrogen beam begins to be injected. The hydrogen beam energy is taken as 180 keV and power as 2.0 MW (deposition power), corresponding to case (i) shown in Figs. 3 and 4. The proton distribution function forms gradually after the high-purity hydrogen beam injection. The energetic protons continuously knock the bulk deuterons to the energetic region; thus, the knock-on tail gradually forms in the deuteron distribution function. Figures 6(a) and 6(b) show the power balance of the fast (knock-on) component in the deuteron distribution function as a function of elapsed time after the high-purity hydrogen beam injection. Here, $P^{NES}_{p\rightarrow fast\,d}$ is the power transferred from the proton to fast (knock-on) deuterons through NES; $P^{Coulomb}_{p\rightarrow fast\,d}$, $P^{Coulomb}_{fast\,d\rightarrow bulk\,d}$, and $P^{Coulomb}_{fast\,d\rightarrow bulk\,e}$ are the transferred power from proton to fast deuterons, fast deuterons to bulk deuteron, and fast deuterons to bulk electrons through Coulomb scattering, respectively. The power lost from the plasma is plotted with a blue dotted line. The plasma condition is the same as those in Fig. 5. The parameter ξ in Fig. 6(b) is the ratio of the sum of the heating power densities (solid lines), i.e., $P^{NES}_{p\rightarrow fast\,d} + P^{Coulomb}_{p\rightarrow fast\,d}$, to the sum of lost power densities (dotted lines), i.e., $P^{Coulomb}_{fast\,d\rightarrow bulk\,d} + P^{Coulomb}_{fast\,d\rightarrow bulk\,e}$ + loss. The transferred power from protons to fast deuterons due to NES $P^{NES}_{p\rightarrow fast\,d}$ gradually increases and almost reaches an equilibrium value at 2 s after the high-purity hydrogen beam injection. The power is estimated at approximately 1.8 kW. It is known that most of the proton beam power is transferred to bulk

TABLE II. Plasma and beam conditions for the large helical device experiments.

H-beam pattern	(i) w/o NBI	(ii) NBI#1	(iii) NBI#1 + 3
H-beam deposition power (MW)	0	2.0	3.6
$T_e(0)$ (keV)	7.9	6.5	7.1
$T_e(a/2)$ (keV)	4.0	4.2	4.2
n_e (m^{-3})	0.79×10^{19}	0.83×10^{19}	0.93×10^{19}
τ_n (ms)	35.2 ± 0.13	44.3 ± 0.8	46.8 ± 0.47

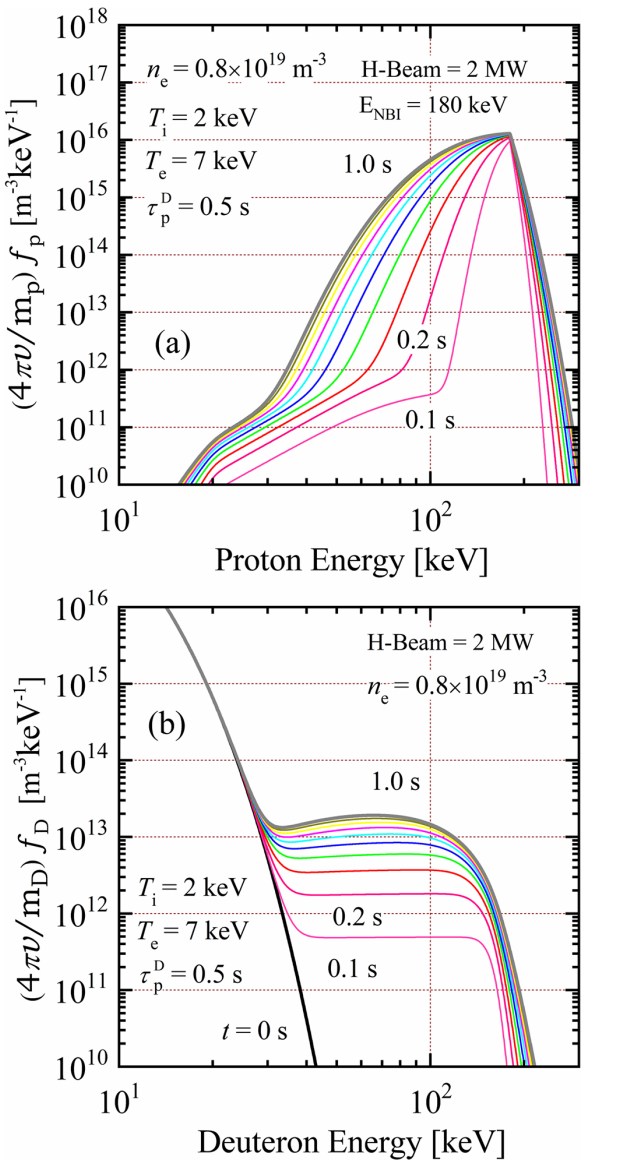

FIG. 5. Time evolutions of (a) proton and (b) deuteron distribution functions after high-purity hydrogen beam was injected with 180 keV energy and 2 MW power.

ions and electrons via Coulomb collisions, i.e., the transferred power to ions (or electrons) is approximately 0.16 (or 0.56) MW in the present simulations; the fraction of transferred power from protons to bulk deuterons via NES to via Coulomb scattering is less than 2% at most. However, it should be noted that the cross section of the D(d,n)^{3}He reaction of the recoil deuteron with a 100 keV energy range is more than four orders larger compared with the typical bulk deuterons. In general thermonuclear fusion plasma, it should be recognized that the small number of fast deuterons sustains the fusion power (neutron) production.

In the experiments shown in Figs. 3 and 4, the hydrogen beam with 50-keV energy and 4.5-MW port-through power, i.e., NBI#5, was injected superimposing on the high-purity hydrogen beam. Almost 50% of hydrogen port-through power penetrated the plasma in the experiment. In general numerical simulations, the fraction of the transparent to port-through (injection) power tends to be larger for the vertical beam injection than for the tangential beam injection. In the present simulation, it is assumed that the deposition power of the vertical beam injection (#NBI5) is almost 50%−60% of the port-through power, i.e., 2 MW. Figure 7 shows the time evolution of (a) proton and (b) deuteron distribution functions after the deuterium beam was turned off, along with (c) deuteron distribution functions when NES was neglected. In the simulation, the confinement time for deuterons is assumed as 0.04 s. The discussion for the confinement time is made later (in Fig. 8). The recoil ions by NES are produced mainly along the proton beamline, which is injected tangentially to the toroidal magnetic axis; thus, the electron temperature at $r = 0$ (center of the plasma) is essential for the recoil ion production (knock-on tail formation). A plasma condition shown in Fig. 4(ii) was selected. During 300 ms after terminating the deuterium beam, the proton distribution function is kept in almost the same shape. In contrast, the beam component in the deuteron distribution function rapidly decays, leaving the residual knock-on tail component. The proton distribution function does not change its shape significantly over time because the hydrogen beam is continuously injected with 180-keV energy and 2-MW power after terminating the deuterium beam injection. In the simulation, the transferred powers due to NES between fast deuteron and field deuteron, fast deuteron and fast deuteron, beam proton and fast deuteron were insignificant in current discussion, because the fast deuteron population is much smaller compared with fast protons.

From the proton and deuteron distribution functions shown in Fig. 7, the transferred energy per unit time from protons to fast deuterons (which are about to slow down) can be evaluated by Coulomb scattering and NES processes at each time step. Figure 8 shows the results as a function of the elapsed time after terminating the

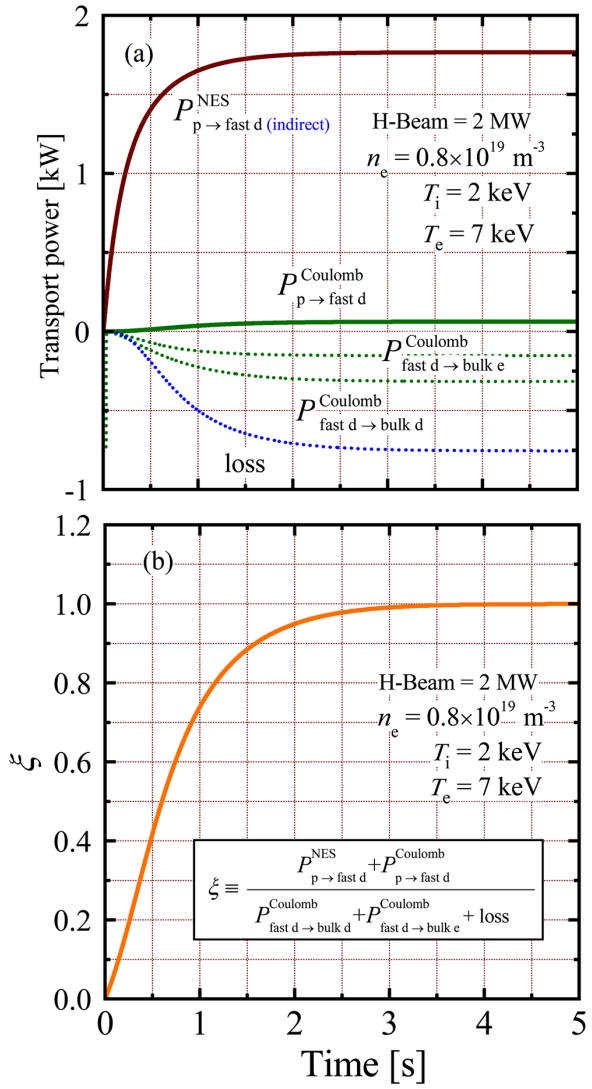

FIG. 6. Time evolution of (a) heating and lost power balanced for knock-on deuteron component and (b) ratio of received and lost powers after high-purity hydrogen beam was injected with 180 keV energy and 2 MW power.

deuterium beam. The green line represents the time evolution of the transferred energy per unit time from protons to slowing-down fast (beam plus knock-on) deuterons through Coulomb scattering. The red line represents the transferred energy through NES (the dotted line represents the total value of the green and red lines). The energy transferred from protons to the fast (beam plus knock-on) component in the deuteron distribution function through Coulomb scattering decreased rapidly. This is because the number of fast deuterons produced by external beam injection (NBI#5) reduces immediately after deuterium beam termination [Fig. 7(b)]. This reduction is because of the slowing-down and loss process of deuterons from the plasma. In contrast, the energy transferred from the protons to fast deuterons through NES is nearly constant for 100 ms. This is because proton and bulk deuteron distribution functions (Maxwell component) do not

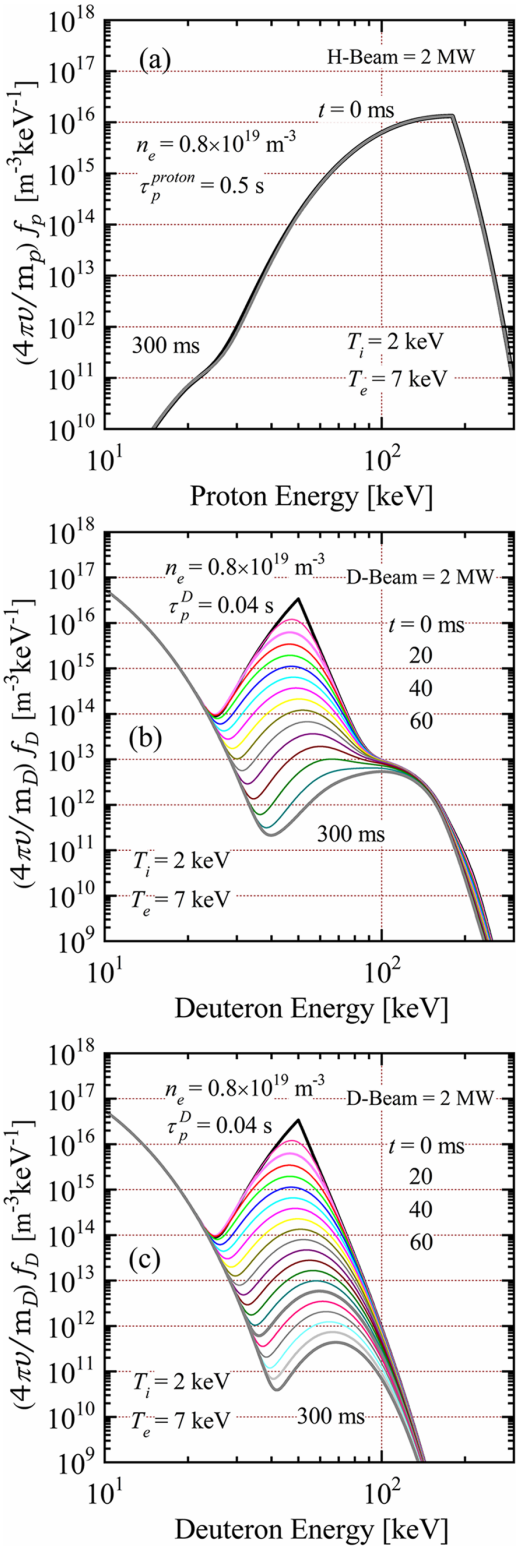

FIG. 7. Time evolutions of (a) proton and deuteron distribution functions when (b) NES is considered and (c) neglected, during 300 ms period after the deuterium beam was terminated.

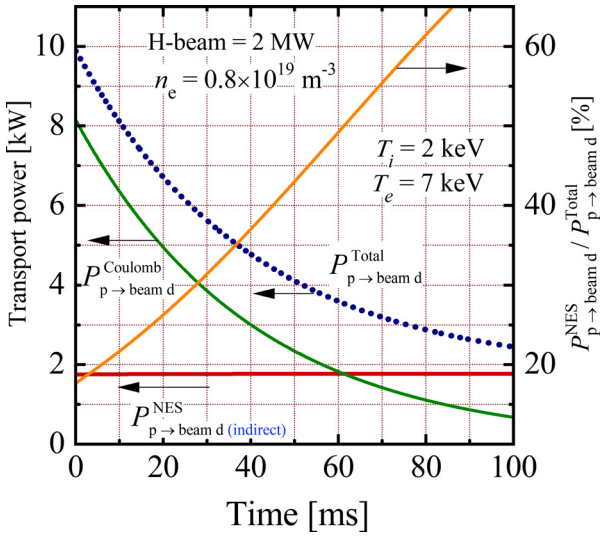

FIG. 8. Time evolution of the transferred power from protons to energetic deuterons via (1) Coulomb scattering and (2) NES, along with the total value (dotted line). The plasma condition is the same as shown in Fig. 4(ii).

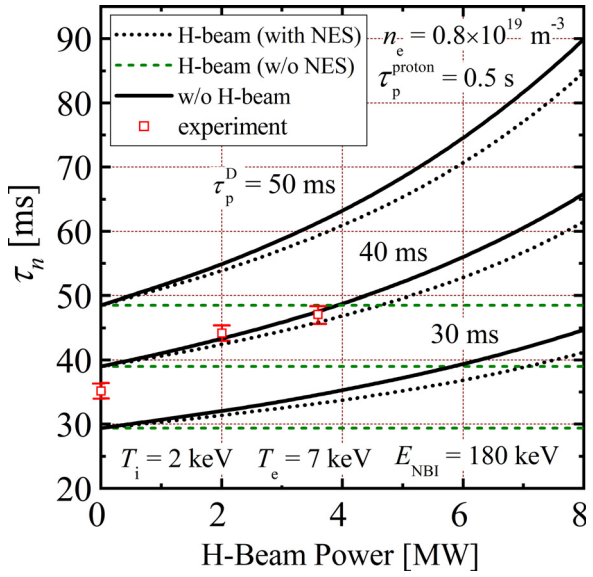

FIG. 9. Neutron decay times when (1) high-purity hydrogen beam is injected, i.e., NES considered (solid line) and neglected (black dotted line), and (2) high-purity hydrogen beam is not injected (green dashed line) as a function of the high-purity hydrogen beam injection powers. The observed experimental values are plotted as red squares.

change their shapes throughout 100 ms, as discussed previously. The energy is transferred through NES from energetic protons to the bulk deuterons. However, the energy is apparently transferred from energetic protons to fast deuterons since the bulk deuterons that received energy are scattered to the energetic region. This energy transfer channel is called "an indirect energy transfer channel." The right-side axis in Fig. 8 represents the ratio of the energy transferred through NES per unit of time to the total energy transferred. The fraction gradually increased and reached 50% at approximately 60 ms after terminating the deuterium beam. Although the NES cross section of protons with 180 keV hydrogen beam energy is significantly smaller than that of the Coulomb one, the NES processes occur between energetic protons and bulk deuterons (the Coulomb scattering process occurs between energetic protons and fast deuterons). The magnitude of the transferred energies through Coulomb scattering and NES processes could become comparable because the bulk component of the deuteron distribution function is several orders of magnitude larger than the fast deuteron component. Thus, we could observe the phenomena induced by NES in the LHD.

Additional BFP simulations were made by changing the high-purity hydrogen beam injection powers and deuteron confinement times, and for each plasma condition, the decay times of the neutron generation rates were evaluated. The results are shown in Fig. 9, where the neutron decay times estimated through the BFP simulation are plotted as a function of the hydrogen beam power for several deuteron confinement times. The solid lines represent the neutron decay time when the NES effect is considered, whereas the dotted (black) lines represent the decay time when the NES effect is neglected. The dashed (green) lines indicate the decay time when the hydrogen beam was not injected. The background plasma conditions were chosen by roughly averaging the experimental condition shown in Table II, i.e., $T_i = 2$ keV, $T_e = 7$ keV, $n_e = 0.8 \times 10^{19}$ m^{-3}, $E_{NBI} = 180$ keV, and $\tau_p = 0.5$ s. The ion temperature and electron density are almost radially flat, so we used radial average values in the simulation. Since the proton beam was injected tangentially to the magnetic axis and most knock-on tail would be generated around the central region, we chose the average electron temperature around the central region. The red squares represent the decay time observed in the LHD experiments shown in Table II. During the neutron decay process shown in Fig. 4, the plasma temperature (or density) is fluctuated about 8% (or 10%) from the averaged value at the maximum. The sensitivities of the plasma parameters on the neutron decay time are estimated using the BFP model for the experimental condition shown in Table II-ii ($\tau_p^D = 40$ ms case in Fig. 9), and the results are summarized in Table III. The fluctuations of the neutron decay time caused by the plasma temperature or density can be estimated less than 1.8%. Since the particle loss from the plasma is influential in the current plasma condition, the sensitivities may be smaller compared with the previous prediction not considering the particle loss from the plasma.[20,21] The errors for the least squares fitting shown in Table II are also estimated less than 1.6%; in addition, counting errors in FC are considered less than 0.4%;[12] thus, we have drawn error bars roughly within ±3% in the neutron decay times observed in the experiment in Fig. 9. The neutron decay time can be increased in a non-equilibrium state by both

TABLE III. Sensitivity of the plasma parameters on neutron decay time τ_n (ms).

ΔT_e or Δn_e	−10%	0	+10%
T_i sensitivity	43.1 (−0.5%)	43.3	43.4 (+0.2%)
T_e sensitivity	43.0 (−0.7%)	43.3	43.5 (+0.5%)
n_e sensitivity	43.9 (+1.4%)	43.3	42.6 (−1.6%)

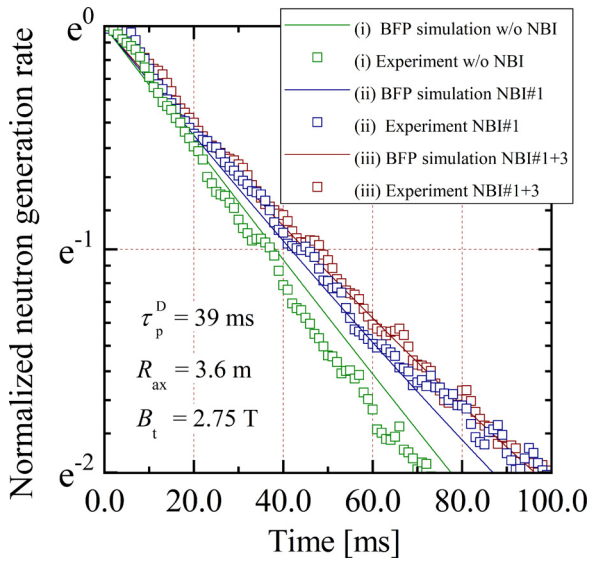

FIG. 10. Comparison of the neutron decay process between observed data (see Table II and Fig. 4) and BFP simulations when deuteron confinement time is assume as 39 ms.

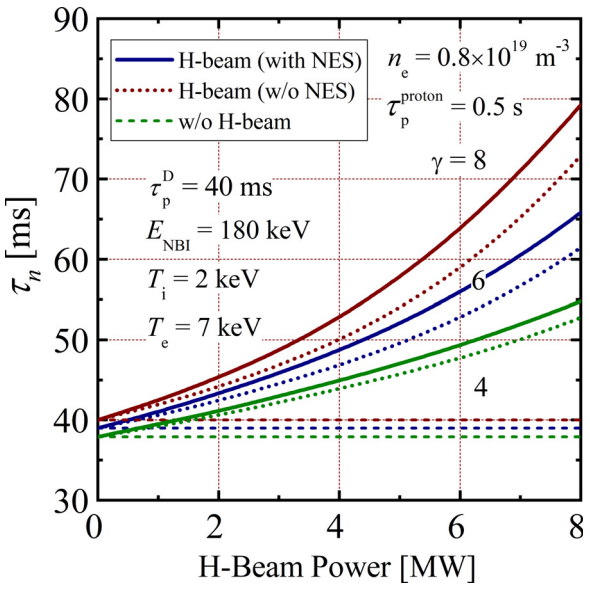

FIG. 11. Neutron decay times when (1) high-purity hydrogen beam is injected, i.e., NES considered (solid line) and neglected (black dotted line), and (2) high-purity hydrogen beam is not injected (green dashed line) as a function of the high-purity hydrogen injection powers for several γ values.

Coulomb scattering and NES processes, even if the beam energy is in approximately 180 keV, as discussed previously. The BFP simulation model explains the experimental data within a realistic range if the deuteron confinement time is set to around 40 ms. In this case, the energy transferred per unit time from protons to fast deuterons through NES is approximately 1.8 kW, which is the same order with the one through the Coulomb scattering, i.e., approximately 3–8 kW. Consequently, a delay in the deuteron slowing-down time (delay in the neutron decay time) would be induced and we can observe the phenomena in LHD. In Fig. 10, the neutron decay times evaluated by the BFP simulations for the plasma conditions shown in Table II are compared with the observed data. Here, the deuteron confinement time is set to 39 ms. The dependency of the γ value defined in Eq. (5) is examined. Figure 11 shows the decay times of the neutron generation rates for different γ values. The solid lines represent the neutron decay time when the NES effect is considered, whereas the dotted (black) lines represent the decay time when the NES effect is neglected. The dashed (green) lines indicate the decay time when the hydrogen beam was not injected. The decay time increases as the γ value increases. This is because the higher γ value ensures a large confinement time for the energetic region. The γ dependency on the NES effect (deviation between solid and dotted line) is quantified, i.e., the deviation for $\gamma = 4$, 6, and 8 are 2.1%, 3.6%, and 4.9% when 3.6 MW hydrogen beam power, respectively.

The NES effect on the D(d,n)^{3}He reactivity for several plasma parameters is predicted for the future fusion device, e.g., JT60-SA. Figure 12 shows the enhanced neutron generation rate due to NES for several (a) electron temperatures, (b) electron densities, and (c) beam injection energies. The default plasma parameters are chosen referencing the shot conditions reported in Ref. 9 (#164874), i.e., $T_i = 2$ keV, $T_e = 12$ keV, $n_e = 10^{19}$ m^{-3}, $E_{NBI} = 170$ keV, and beam deposition power $P_{NBI} = 7$ MW. In this experiment, approximately one order of neutron generation rate was observed as a result of the high-purity hydrogen beam injection. In a brief calculation, the neutron generation in Maxwellian plasma with the above plasma parameter is approximately 10^{11} m^{-3} s^{-1}. As shown in Fig. 12(a), the BFP simulation also reproduces approximately one order of the enhancement in the neutron generations rate for the plasma condition of #164874 in Ref. 9, i.e., $T_e = 12$ keV, which is consistent with the experimental observation. For high electron temperature, the slowing-down of fast ions is weakened; however, energetic components of proton and deuteron distribution functions grow large. Thus, the enhancement of fusion reactivity appears larger for the high electron temperature range. Similarly, the slowing-down of energetic ions is weakened by decreasing electron (ion) density. However, the resulting magnitude of the knock-on tail is not significantly influenced by the electron (ion) density because the number of recoil ions increases in proportion to the increases in the ion density as shown in Fig. 12(b). It is worth noting that the density influences the neutron decay time and the absolute value of the neutron generation rate; thus, an experiment with low-density plasma would be profitable to observe the NES effect since the competitive slowing-down process due to Coulomb scattering decreases in low-density plasma. One important parameter would be the beam injection energy. The transferred energy in a single NES event is increased with an increase in relative velocity. The NES effect becomes essentially significant with increasing relative velocity. As shown in Fig. 12(c), when the beam injection energy increases to 500 keV, the magnitude of the enhancement in the neutron generation rate reaches almost one order larger than that of 170 keV energy. In the LHD experiment, the high-purity hydrogen beam (approximately 170–180 keV) was used to distinguish the recoil deuterons from beam-injected protons. This is because the recoil component is smaller than the beam component. The NES effect for the deuterium beam may be

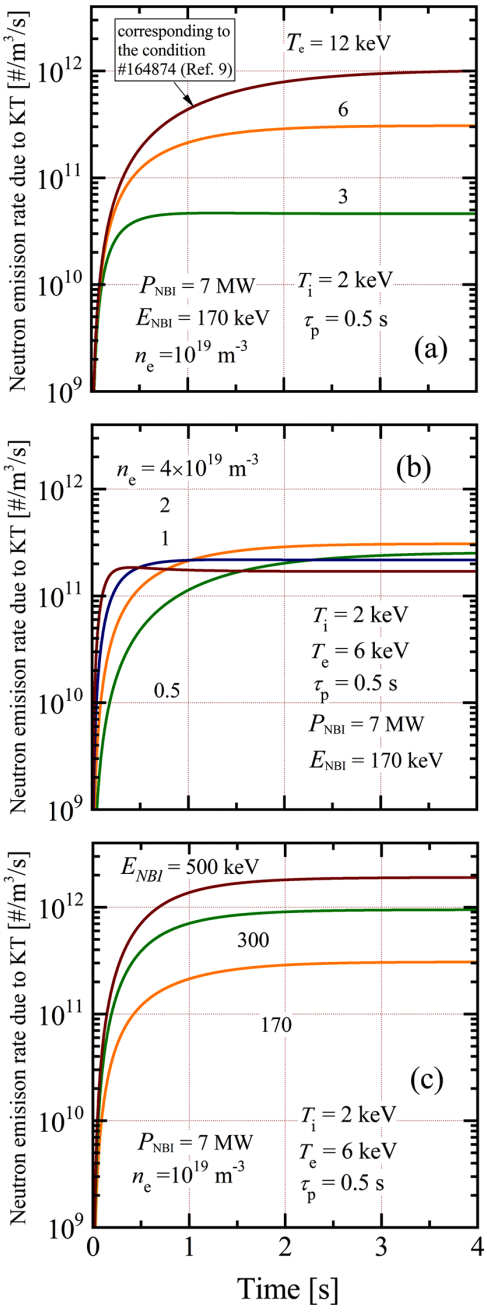

FIG. 12. Time evolution of enhanced D(d,n)^{3}He neutron generation rates due to knock-on tail formation in deuteron distribution function after high-purity hydrogen beam is injected for several (a) electron temperatures, (b) electron densities, and (c) hydrogen beam injection energies.

observed in the experiment with higher beam injection energy. The NES effect essentially becomes important for beam-injected and further energetic fusion-born ions. Therefore, further confirmation using such large beam injection energies would be necessary to predict the NES effects induced by fusion-born energetic ions in the future reactor. The γ dependency on the neutron generation rate is quantified. The neutron generation rate when $\gamma = 4$ (or 8) for $T_i = 2$ keV, $T_e = 6$ keV, $n_e = 10^{19} \times$ m^{-3}, $E_{NBI} = 170$ keV, and beam deposition power $P_{NBI} = 7$ MW is 2.82 (or 3.22) $\times 10^{11}$ m^{-3} s^{-1}; the difference from the neutron generation rate (3.07×10^{11} m^{-3} s^{-1}) when $\gamma = 6$ [yellow lines in Figs. 12(a)–12(c)] is evaluated as −8.1 (4.9)%. The deviation of the neutron generation rate due to γ value is insignificant compared with the magnitude of the enhancement due to the knock-on tail formation.

V. CONCLUDING REMARKS

In this study, the transferred power was estimated using NES between energetic ions to adapt to the data observed in LHD, i.e., the delay process of the neutron decay time induced by the delay in the deuteron slowing-down process. By considering an indirect energy transfer channel induced by recoil ions, which receive the energy from fast ions via NES, the reactivity enhancement observed in the LHD can be explained. The BFP simulations reproduced the experimental data with adjustment parameters (fast deuteron confinement time, and its velocity dependency, i.e., γ parameter). It is shown that the transferred energy due to NES per unit time could reach the same order as the one due to Coulomb scattering, even if the beam injection energy is 180 keV.

Isotropic plasma was assumed throughout the simulations, and the transferred power due to NES was roughly evaluated. In the LHD experiments, the directions of deuterium and hydrogen beams to the toroidal magnetic field were different, which might induce the difference in the scattering process compared with the isotropic model. The average relative speed between the tangential and vertical injection beams becomes larger than that of the isotropic one; thus, the Coulomb scattering frequency tends to decrease, and the NES frequency increases slightly. In the comparison between observed data and simulations, errors caused by the radial profiles of plasma density and temperature might be included. For detailed evaluation, more sophisticated simulations considering the anisotropy of the plasma would be necessary. Currently, the analysis using the particle simulation code considering the NES phenomena is developing.[22] The discussion including anisotropic effects will be made in the subsequent analysis. The NES effect becomes more significant as the beam injection energy increases. In such a case, the fraction of the transferred energy via NES increases, and the energy range where recoil ions appear is shifted to the high-energy side. Confirmation of the scaling of the NES with injection energy will require further experiments with high energy NBI.

ACKNOWLEDGMENTS

The authors would like to thank the cooperative program of No. NIFS20KLPH047 and the LHD experimental group for their contributions. The first author is grateful to Emeritus Professor Y. Nakao for his discussions and encouragement over the course of many years.

AUTHOR DECLARATIONS

Conflict of Interest

The authors have no conflicts to disclose.

Author Contributions

Hideaki Matsuura: Conceptualization (lead); Formal analysis (lead); Investigation (equal); Project administration (lead); Writing – original draft (lead). **Masaki Osakabe:** Conceptualization (equal); Data curation (equal); Funding acquisition (equal); Investigation (equal); Project administration (equal). **Takeo Nishitani:** Conceptualization (equal); Data curation (equal); Investigation (equal); Project administration (equal); Validation (equal). **Shota Sugiyama:** Conceptualization (equal); Investigation (equal); Validation (equal). **Kento Kimura:** Investigation (equal); Validation (equal). **Daisuke Umezaki:** Investigation (equal); Validation (equal). **Kunihiro Ogawa:** Conceptualization (supporting); Data curation (equal); Funding acquisition (equal); Investigation (equal); Project administration (equal); Validation (equal); Writing – review & editing (equal). **Mitsutaka Isobe:** Conceptualization (equal); Data curation (equal); Funding acquisition (equal); Investigation (equal); Project administration (equal); Validation (equal); Writing – review & editing (equal). **Yasuko Kawamoto:** Data curation (equal); Investigation (equal); Validation (equal). **Tetsutarou Oishi:** Data curation (equal); Investigation (equal). **Motoshi Goto:** Data curation (equal); Investigation (equal). **Naoki Tamura:** Data curation (equal); Investigation (equal).

DATA AVAILABILITY

The LHD data can be accessed from the LHD data repository at https://www-lhd.nifs.ac.jp/pub/Repository_en.html.[23]

REFERENCES

[1]J. J. Devaney and M. L. Stein, Nucl. Sci. Eng. **46**, 323 (1971).
[2]J. Galambos, J. Gilligan, E. Greenspan, P. Stroud, and G. H. Miley, Nucl. Fusion **24**, 739 (1984).
[3]Y. Nakao, H. Hori, T. Hanada, K. Kudo, and M. Ohta, Nucl. Fusion **28**, 1029 (1988).
[4]S. T. Perkins and D. E. Cullen, Nucl. Sci. Eng. **77**, 20 (1981).
[5]L. Ballabio, G. Gorini, and J. Källne, Phys. Rev. E **55**, 3358 (1997).
[6]J. Källne, L. Ballabio, J. Frenje, S. Conroy, G. Ericsson, M. Tardocchi, E. Traneus, and G. Gorini, Phys. Rev. Lett. **85**, 1246 (2000).
[7]A. A. Korotkov, A. Gondhalekar, and R. J. Akers, Phys. Plasmas **7**, 957 (2000).
[8]H. Matsuura, S. Sugiyama, K. Kimura, S. Kajimoto, T. Nishitani, K. Ogawa, Y. Kawamoto, M. Isobe, and M. Osakabe, Nucl. Fusion **60**, 066007 (2020).
[9]H. Matsuura, K. Kimura, D. Umezaki, K. Ogawa, M. Isobe, T. Nishitani, Y. Kawamoto, T. Oishi, M. Goto, M. Osakabe, and S. Sugiyama, Nucl. Fusion **61**, 094001 (2021).
[10]H. Matsuura and Y. Nakao, Phys. Plasmas **13**, 062507 (2006).
[11]M. Osakabe, M. Isobe, M. Tanaka, G. Motojima, K. Tsumori, M. Yokoyama, T. Morisaki, Y. Takeiri, and LHD Experiment Group, IEEE Trans. Plasma Sci. **46**, 2324 (2018).
[12]M. Isobe, K. Ogawa, T. Nishitani, N. Pu, H. Kawase, R. Seki, H. Nuga, E. Takada, S. Murakami, Y. Suzuki *et al.*, Nucl. Fusion **58**, 082004 (2018).
[13]H. Matsuura, M. Nakamura, O. Mitarai, and Y. Nakao, Plasma Phys. Controlled Fusion **53**, 035023 (2011).
[14]M. M. Rosenbluth, W. M. Macdonald, and D. L. Judd, Phys. Rev. **107**, 1 (1957).
[15]D. E. Cullen and S. T. Perkins, Nucl. Sci. Eng. **81**, 75 (1982).
[16]Y. Nakao, T. Honda, K. Kudo, T. Shiba, and H. Nakashima, Nucl. Fusion **30**, 143 (1990).
[17]E. Bittoni, J. G. Cordey, and M. Cox, Nucl. Fusion **20**, 931 (1980).
[18]H. Nuga, R. Seki, K. Ogawa, S. Kamio, Y. Fujiwara, M. Osakabe, M. Isobe, T. Nishitani, M. Yokoyama, and LHD Experiment Group, Plasma Fusion Res. **14**, 3402075 (2019).
[19]H.-S. Bosch and G. M. Hale, Nucl. Fusion **32**, 611 (1992).
[20]J. D. Strachan, P. L. Colestock, S. L. Davis, D. Eames, P. C. Efthimion, H. P. Eubank, R. J. Golodston, L. R. Grisham, R. J. Hawaryluk, K. C. Hosea, J. Hovey, D. L. Jassby, D. W. Johnson, A. A. Mirin, G. Schilling, R. Stooksberry, L. D. Stewart, and H. H. Towner, Nucl. Fusion **21**, 67 (1981).
[21]T. Nishitani, K. Ogawa, N. PU, H. Kawase, S. Murakami, M. Isobe, M. Osakabe, and LHD Experimental Group, Plasma Fusion Res. **13**, 3402024 (2018).
[22]H. Matsuura, S. Sugiyama, S. Kajimoto, D. Sawada, Y. Nishimura, and Y. Kawamoto, Plasma Fusion Res. **11**, 1403105 (2016).
[23]"LHD Experiment Data Repository, operated by NIFS, 2021", see https://www-lhd.nifs.ac.jp/pub/Repository_en.html.